Supplemental Figures

Supplemental Figure 1. CK2a selectively phosphorylates the NRID domain of NCoR.

(A) HeLa cells were transfected with various deletion mutants of FLAG-tagged NCoR plasmids. Whole cell lysates were immunoprecipitated with CK2a antibody and subsequently immunoblotted with the indicated antibodies. (B) GST-pull down assays were performed with indicated GST-NCoR proteins and in vitro translated CK2a or CK2b. Bound proteins were eluted and analyzed by autoradiography. (C) In vitro kinase assays were performed by incubation of various GST-NCoR proteins and recombinant CK2a. The samples were processed for SDS-PAGE and subsequently visualized by autoradiography. (D) TBB inhibits the CK2-mediated phosphorylation of NCoR-15/16. In vitro kinase assays were performed with recombinant CK2a in the presence or absence of increasing amounts of TBB (10, 50, 100 mM). The samples were processed for SDS-PAGE and subsequently visualized by autoradiography. (E) Either FLAG-NCoR-15/16 or Myc-CK2a was transfected into HeLa cells in the presence or absence of TBB (50 mM, 6 hr). Whole cell lysates were immunoprecipitated with anti-FLAG antibody and subsequently immunoblotted with the indicated antibodies.

Supplemental Figure 2. CK2α directly phosphorylates Ser-2436 of NCoR in vivo.

(A) Prediction of CK2α phosphorylation sites in the NCoR-15/16-3 domain. The NCoR sequence was analyzed by an artificial network predictor (http://www.cbs.dtu.dk/services/NetPhosK/). Phosphorylation sites predicted with high probability are shown in asterisks. (B) Peptide sequences for the generation of the phospho-specific NCoR antibody. (C) FLAG-NCoR 15/16 was transfected into HeLa cells, and cell lysates were analyzed by Western blotting with phospho-specific NCoR antibody in the presence of phosphor- or non-phospho peptide (1 mg/ml). (D) Western blot analysis for the expression of NCoR constructs used for Figure 1G. (E) Control PLA image for Figure 1G with transfection of pSG5 empty vector into HeLa cells.

Supplemental Figure 3. Confirmation of CK2α-mediated NCoR phosphorylation at Ser-2436 by MS analysis.

HeLa cell lysates were immunoprecipitated with IgG or anti-CK2α antibody and subsequently proceeded for in vitro kinase assays using synthesized non-phospho-peptides (CQYETLSDSDD) as substrates. The phosphorylated peptide samples were analyzed by MALDI-TOF. Arrow indicates the phosphorylated form of substrate. Peptide of 1355.38 Da and 1377.35 are phosphorylated form of peptide of 1275.40 Da and 1297.37 Da, respectively. Increment of 80 Da mass indicates addition of molecular weight of phosphate group, $-PO_3$.

Supplemental Figure 4. CK2α-dependent phosphorylation of NCoR is critical for NCoR stability.

(A) HeLa cells were treated with cycloheximide (10 μg/ml) and TBB (50 μM) and/or MG132 for various time periods, and cell lysates were analyzed by Western blotting. (B) HeLa cells were treated with an increasing amount of TBB, emodin and siCK2α, respectively, and then cell lysates were analyzed by Western blotting with indicated antibodies.

Supplemental Figure 5. CK2α suppresses the Siah1-mediated degradation of NCoR.

FLAG-Siah1 and/or Myc-CK2α was transfected into HeLa cells in the presence or absence of TBB (50 mM, 6 hr). Whole cell lysates were immunoblotted with the indicated antibodies.

Supplemental Figure 6. The CK2α activities in both HCE4 and TE2-CK2α cells are higher than in TE2 cells.

In vitro kinase assays were performed by incubation of GST-CS (CK2 consensus sequence) protein and immunoprecipitated CK2α enzyme from TE2, TE2-CK2α and HCE4 cells, and CK2α phosphorylation levels were analyzed by autoradiography and scintillation counter.

Supplemental Figure 7. NCoR promotes the invasion of esophageal cancer cells in a CK2-dependent manner.

HCE4 cells were treated with individual siNCoRs, GFP-NCoR plasmids and/or TBB, and invasion was analyzed by counting cells that migrated through the extracellular matrix layer of Biocoat Matrigel invasion chambers. Cell lysates were analyzed by Western blotting with indicated antibodies.

Supplemental Figure 8. cDNA microarray analysis.

(A) HCE4 cells were treated with indicated siRNAs against NCoR, and invasive growth was analyzed by counting cells that migrated through the extracellular matrix layer of Biocoat Matrigel invasion chambers (upper panel). The protein levels were analyzed by Western blotting as indicated. (B) HCE4 cells were transfected with siRNA against NCoR or CK2α, and then the change in mRNA expression was analyzed by cDNA microarray analysis using the Illumina HumanRef-8 v3 Expression Bead Chip. (A) HCE4 cells were treated with indicated siRNAs, and then the levels of indicated genes were analyzed by RT-PCR.

Supplemental Figure 9. Confirmation of siRNA against NCoR and Snail by real-time PCR analysis.

HCE4 cells were transfected with siRNAs. Two days after transfection, cells were harvested, and mRNAs were analyzed by real-time PCR.

Supplemental Figure 10. Overexpression of CK2α inhibits the transcription of IP-10 and E-cadherin genes in TE2 cells.

TE2 cells were transfected with CK2α plasmids and the levels of the indicated genes were analyzed by real-time PCR.

Supplemental Figure 11. The c-Jun-dependent association of NCoR/HDAC3 complex with the API site but not coding region of IP-10 gene.

HCE4 cells were treated with either siNCoR (A) or sic-Jun (B), and ChIP assays were performed with the indicated antibodies. The precipitated samples were analyzed by real-time PCR, and results are given as the percentage of input as means ± SD of three independent experiments.

Supplemental Figure 12. Depletion of NCoR inhibits the CK2α-enhanced invasiveness of TE2 cells.

HCE4 cells were labeled with Fluoresbrite carboxylate nanospheres (Polysciences, Inc.), and then were cultured on the CAM of 11-day-old chick embryos for 3 days. Invasion was monitored in cross-sections of the fixed CAM by fluorescence microscopy.

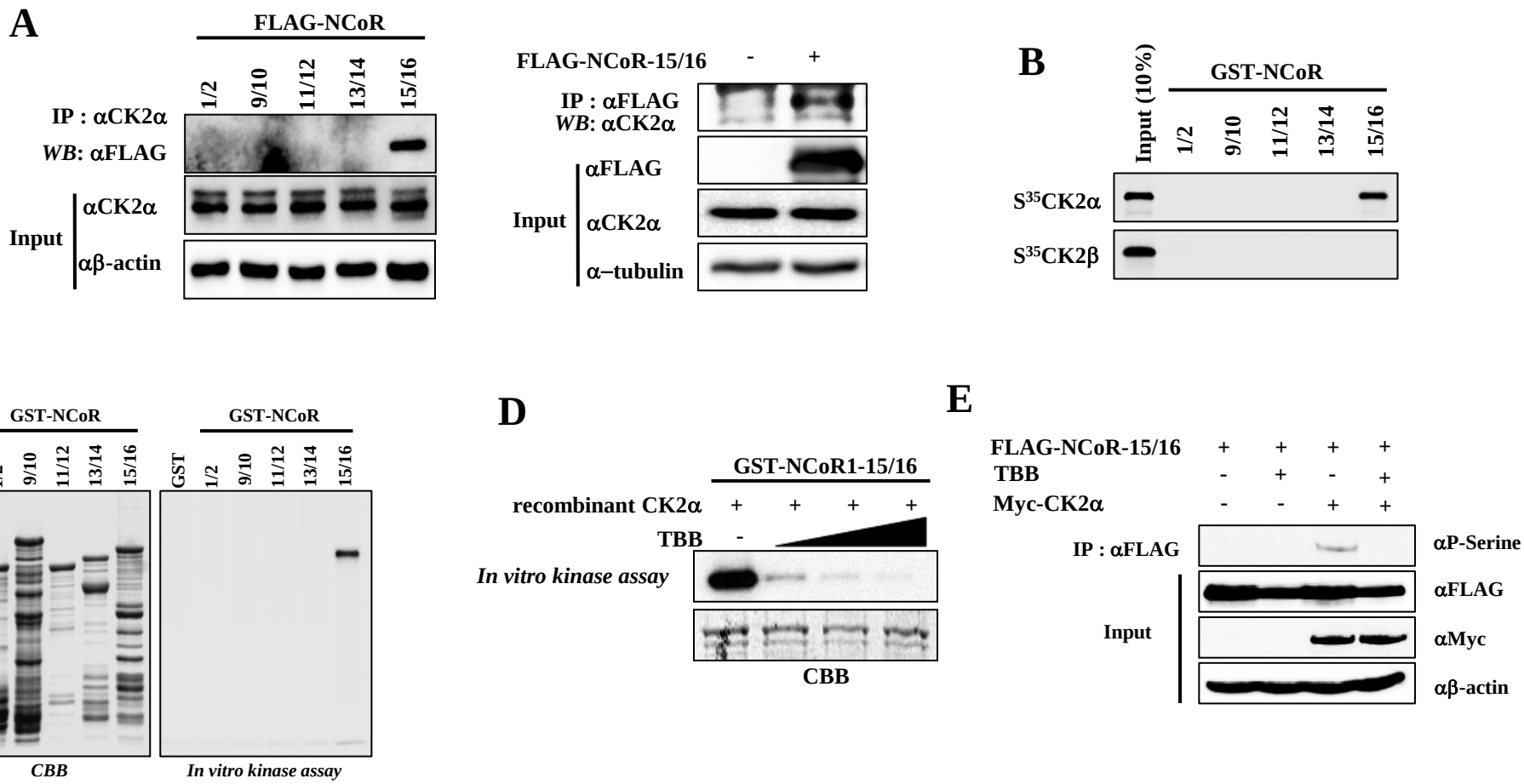

Supplemental Fig. 1. Yoo. et. al

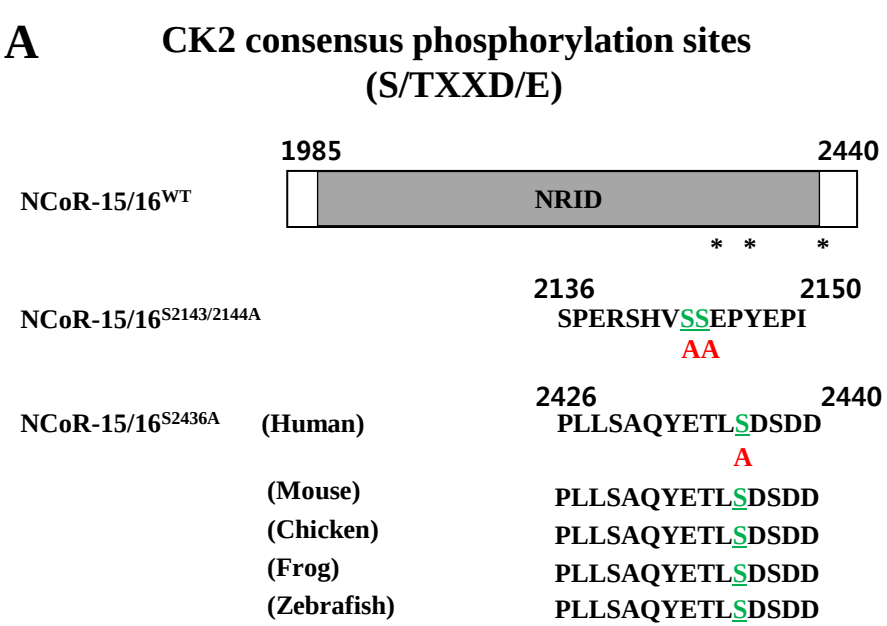

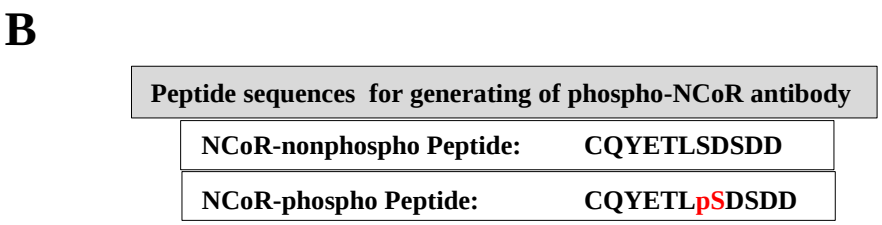

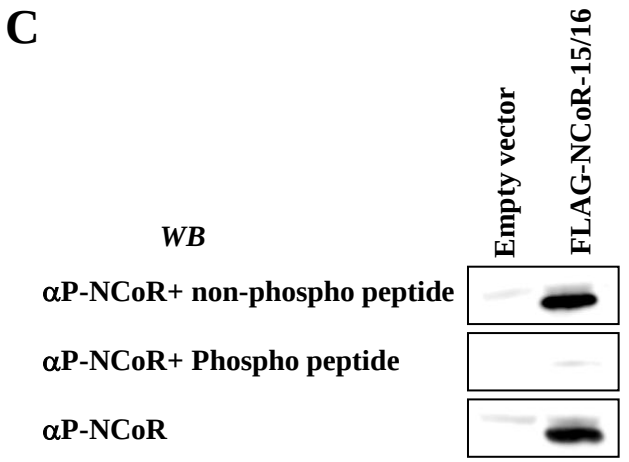

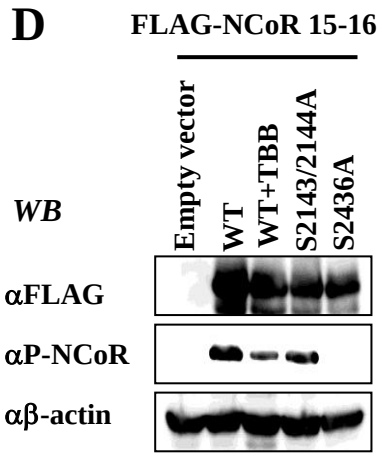

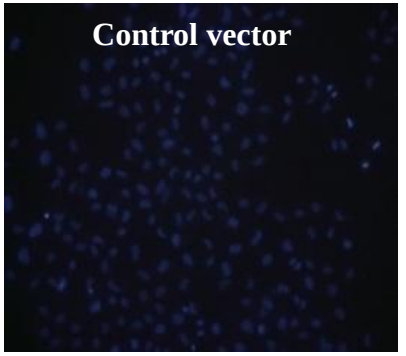

Supplemental Fig. 2. Yoo. et. al

MS spectrum

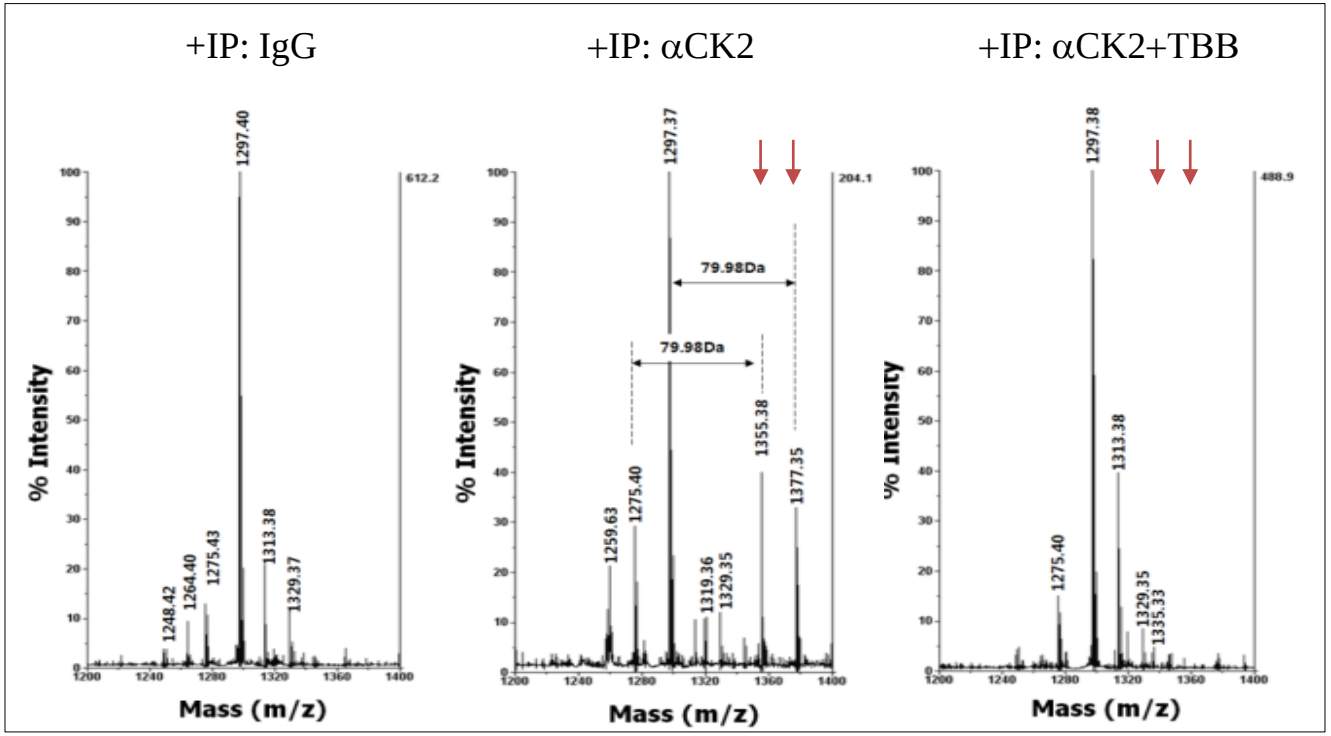

Supplemental Fig. 3. Yoo. et. al

A

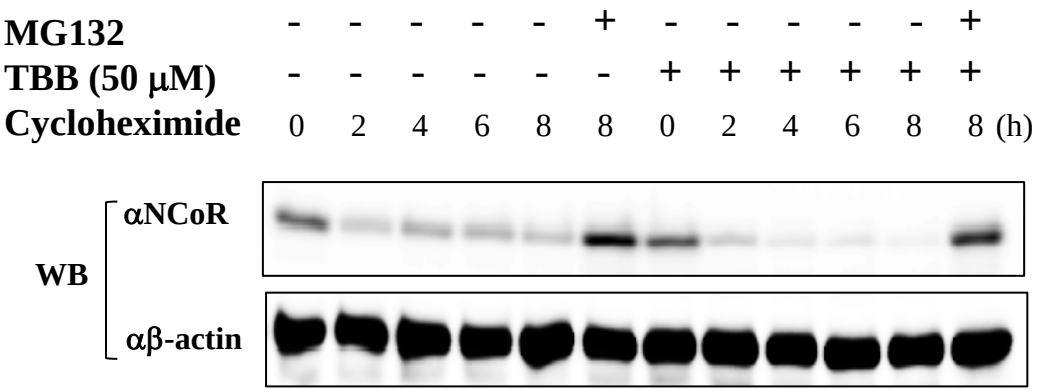

B

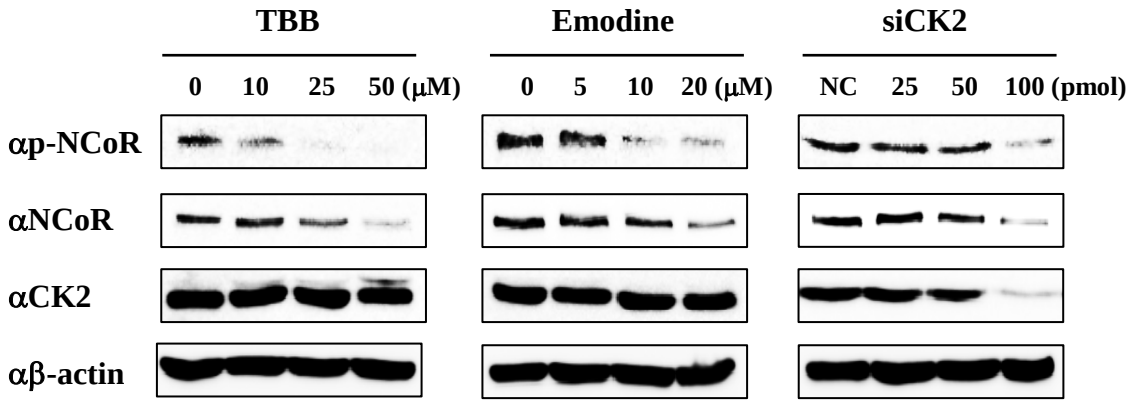

Supplemental Fig. 4. Yoo. et. al

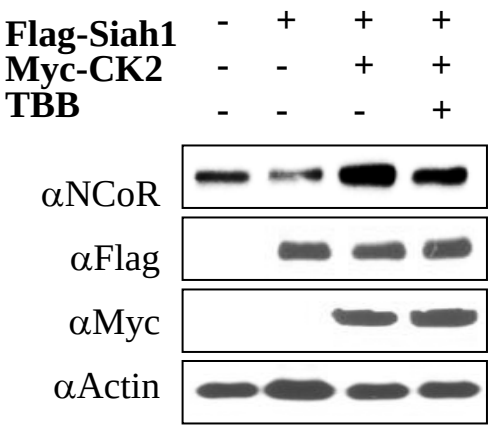

Supplemental Fig. 5. Yoo. et. al

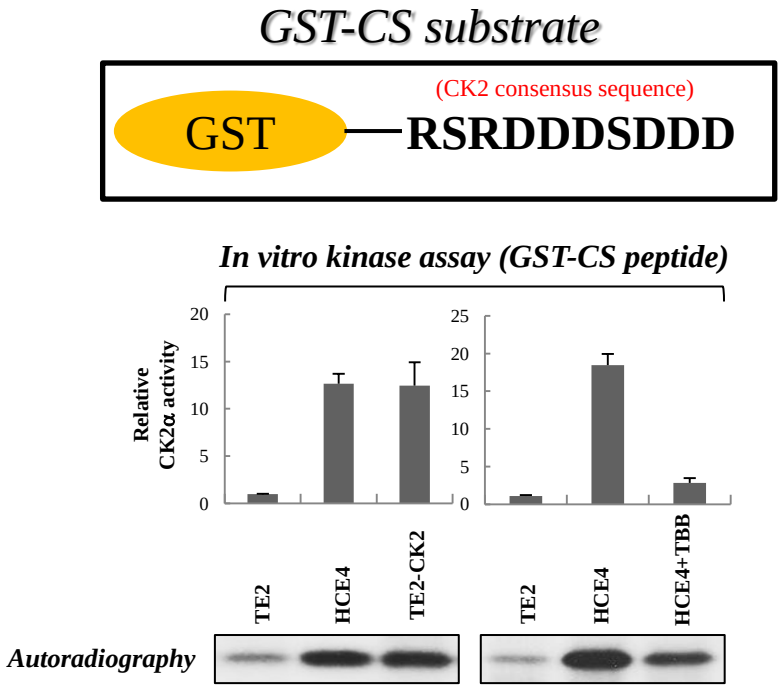

Supplemental Fig. 6. Yoo. et. al

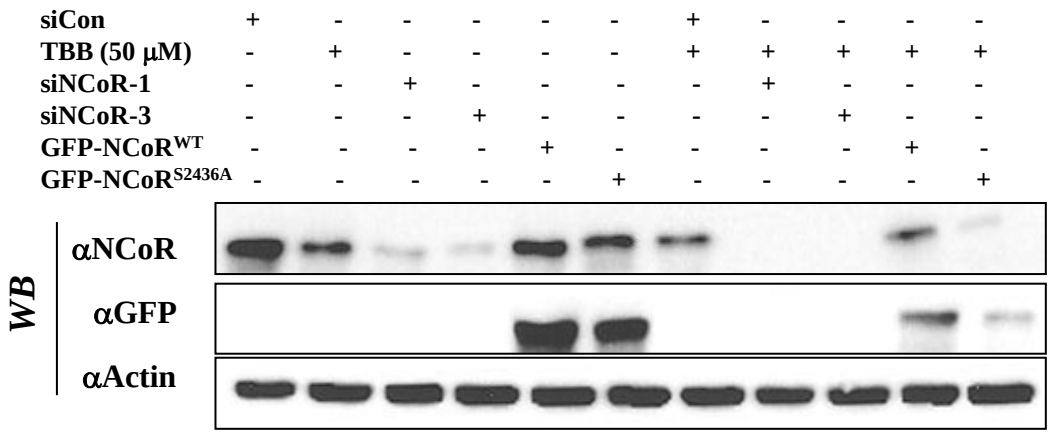

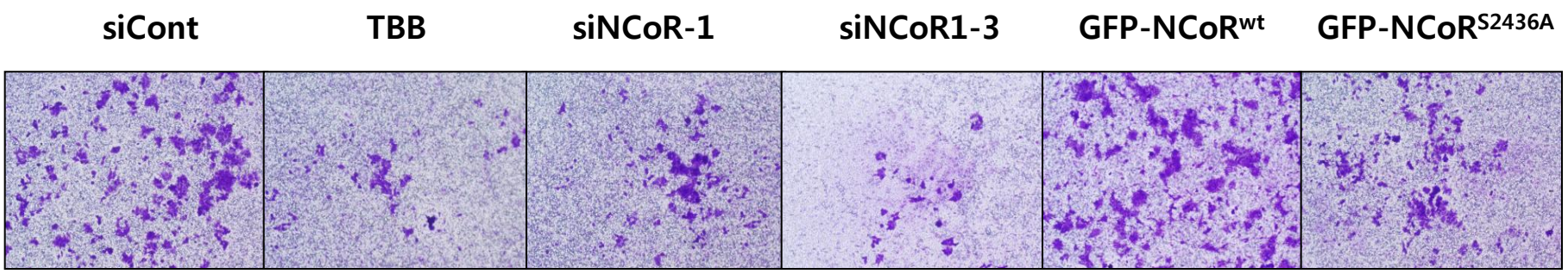

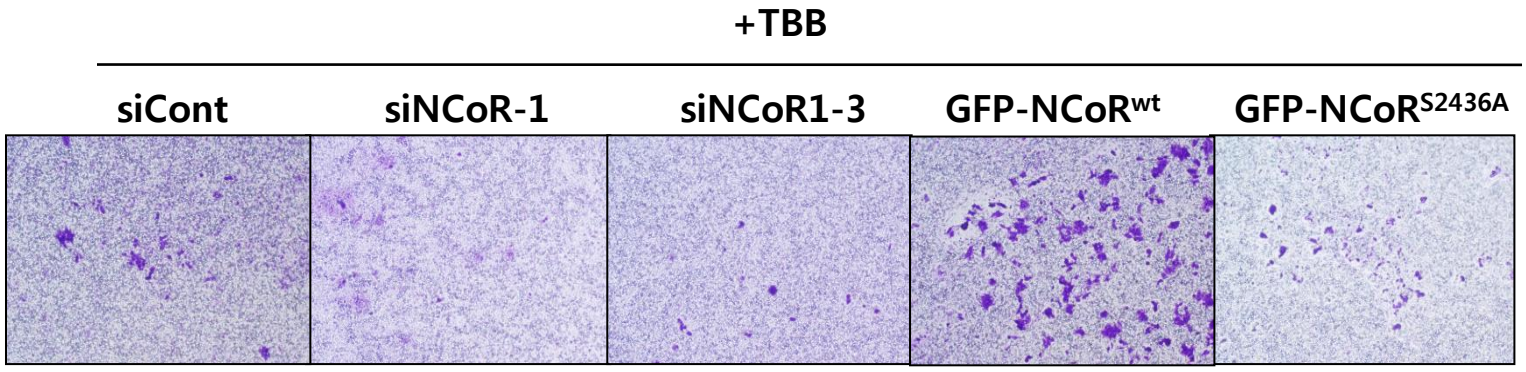

Supplemental Fig. 7. Yoo. et. al

A

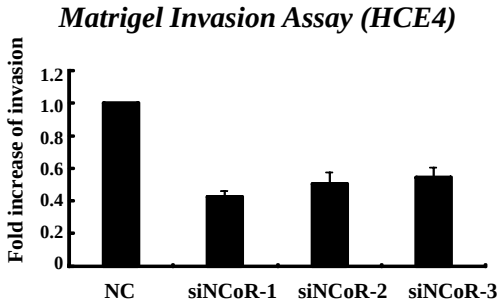

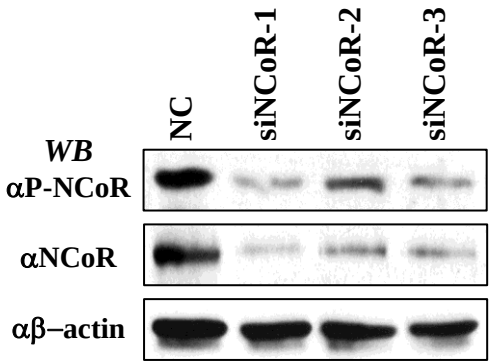

B

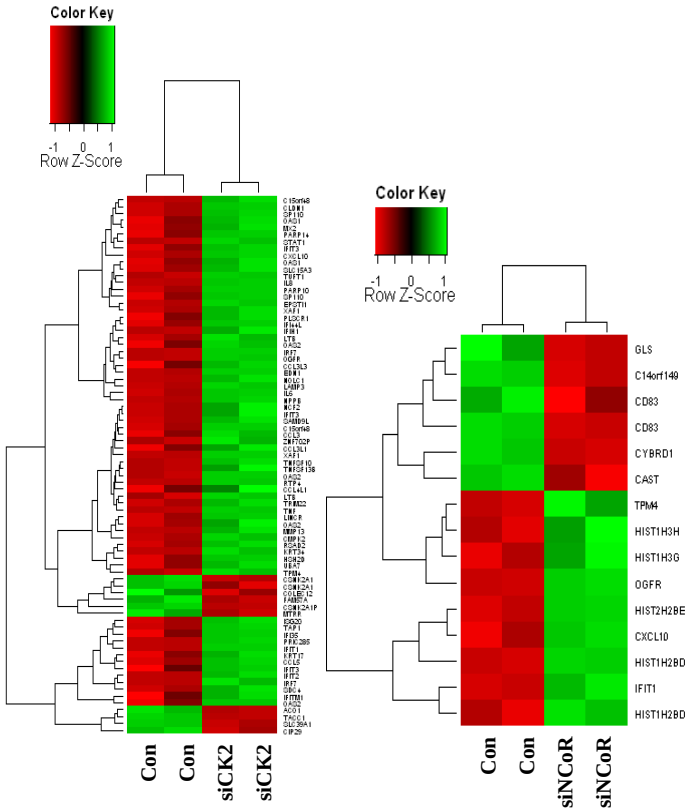

C

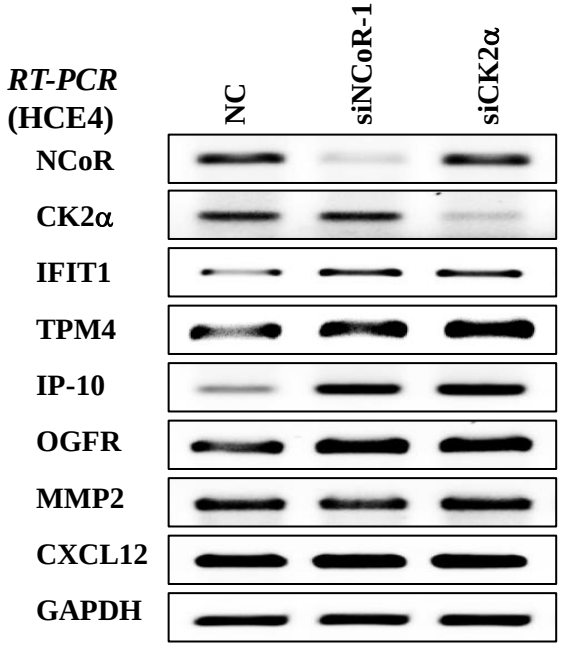

CK2-NCoR putative target genes

Gene name	Accession	Fold exchanges	
		siCK2	siNCoR-1
TPM4	NM_003290.1	2.03	2.06
OGFR	NM_007346.2	2.31	2.18
IFIT1	NM_001548.3	3.18	2.01
IP-10	NM_001565.2	4.22	3.19

Supplemental Fig. 8. Yoo. et. al

Real-time PCR analysis

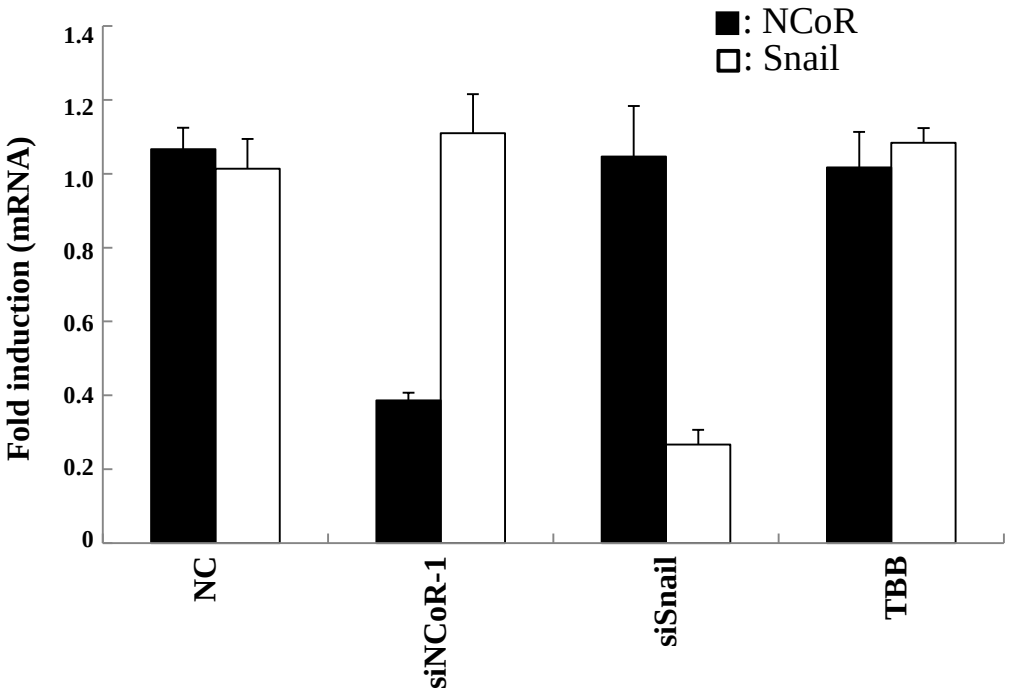

Supplemental Fig. 9. Yoo. et. al

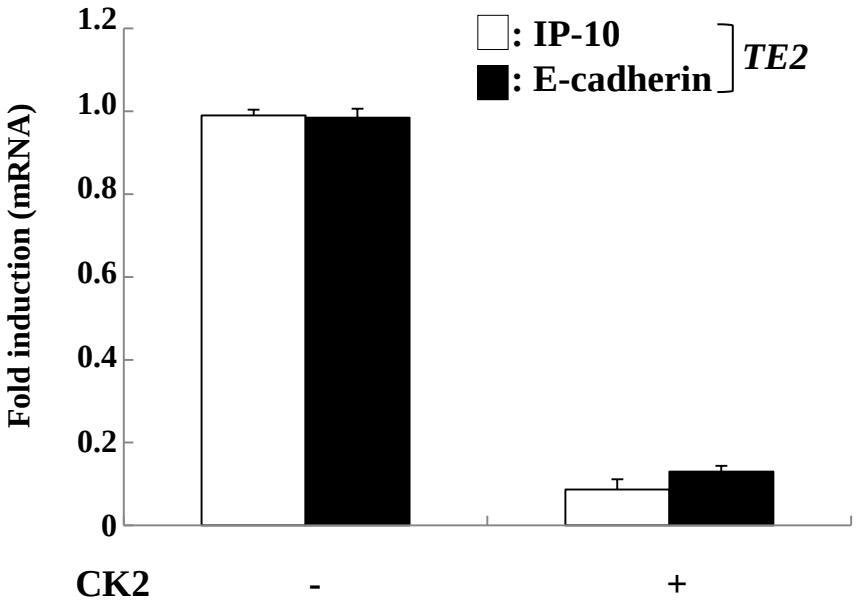

Supplemental Fig. 10. Yoo. et. al

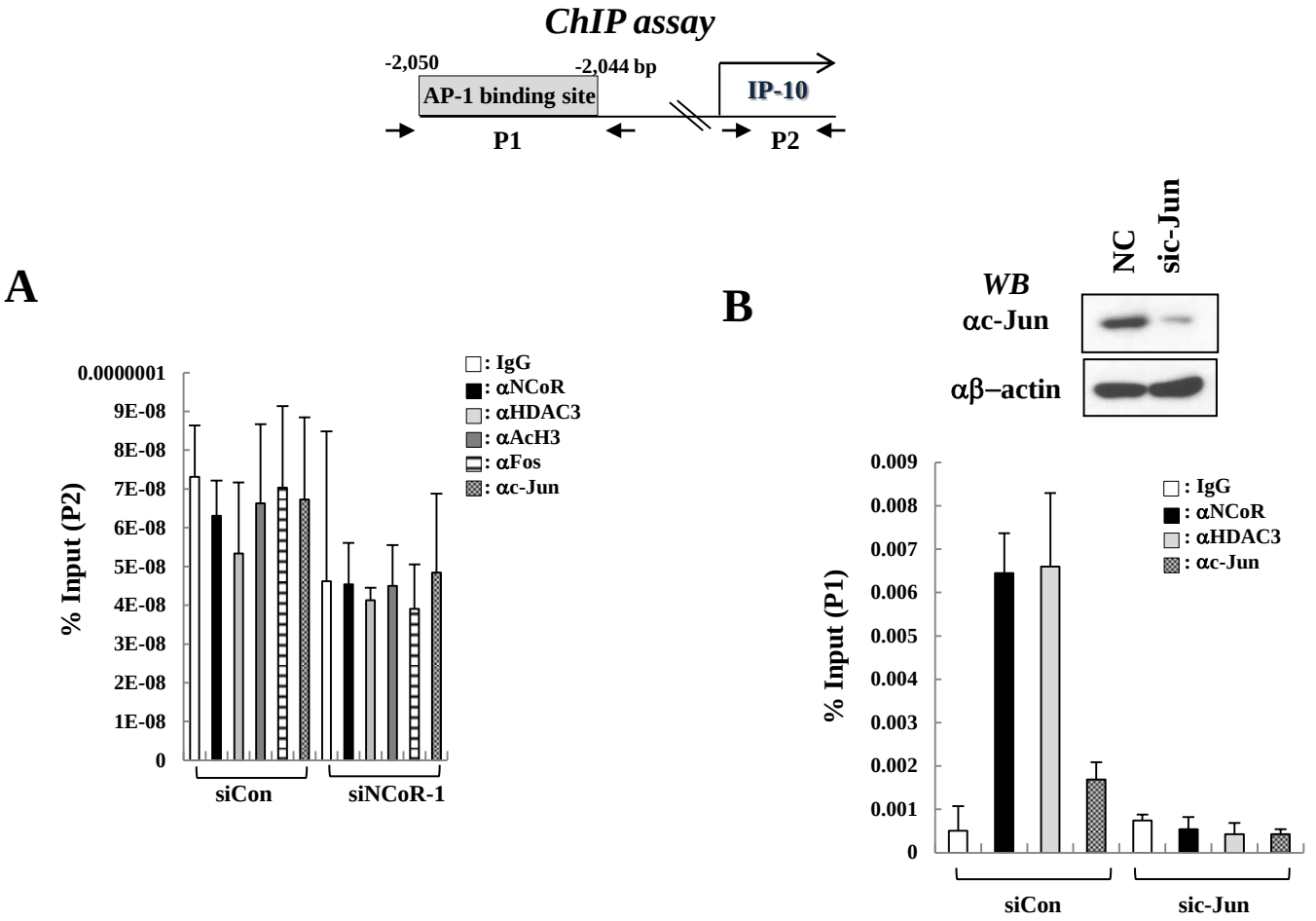

Supplemental Fig. 11. Yoo. et. al

CAM assay (TE2-CK2α)

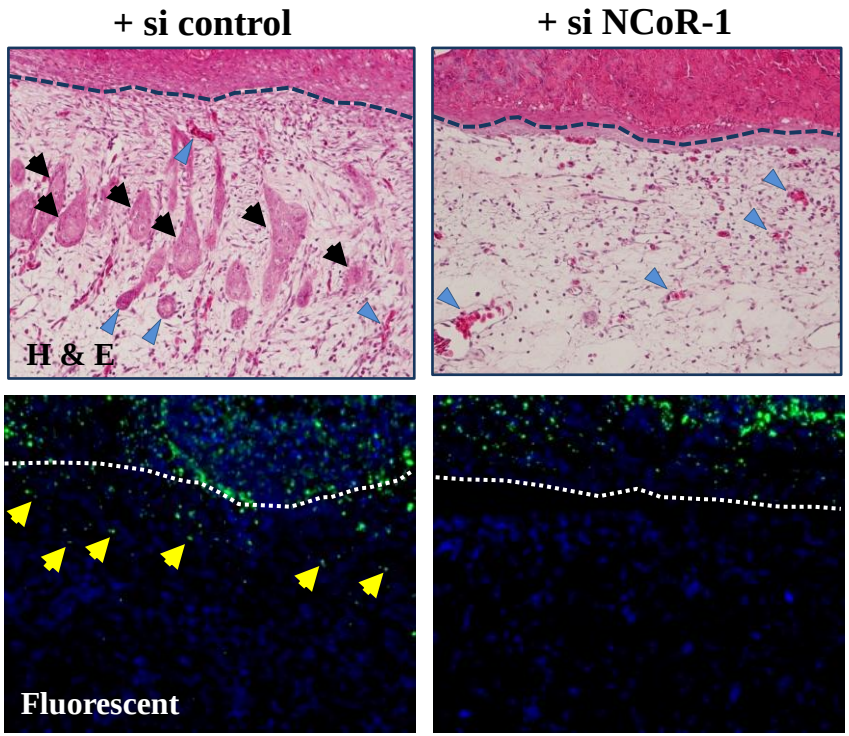

Supplemental Fig. 12. Yoo. et. al